

NP-10-0016  
August 16, 2010

10 CFR 52, Subpart A

U. S. Nuclear Regulatory Commission  
ATTN: Document Control Desk  
Washington, DC 20555-0001



Subject: Exelon Nuclear Texas Holdings, LLC  
Victoria County Station  
Response to Request for Additional Information Letter No. 01  
NRC Docket No. 52-042

References: (1) Exelon Nuclear Texas Holdings, LLC letter to USNRC, Application for Early Site Permit for Victoria County Station, dated March 25, 2010

Exelon Nuclear Texas Holdings, LLC (Exelon) submitted an application for an early site permit (ESP) in Reference 1 for the Victoria County Station (VCS) site.

On July 2, 2010, the NRC requested additional information (RAI) to support the review of certain portions of the VCS ESP application. The letter contained one RAI. The response to the RAI is provided in Enclosure 1:

- RAI Question 02.05.01-1 Basic Geologic and Seismic Information

Regulatory commitments established in this submittal are identified in Enclosure 2. If any additional information is needed, please contact David J. Distel at (610) 765-5517.

I declare under penalty of perjury that the foregoing is true and correct. Executed on the 16<sup>th</sup> day of August, 2010.

Respectfully,

A handwritten signature in black ink that reads 'Marilyn C. Kray'.

Marilyn C. Kray  
Vice President, Nuclear Project Development

DOB7  
NRO

August 16, 2010  
U. S. Nuclear Regulatory Commission  
Page 2

Enclosure: (1) Response to NRC RAI Letter No. 01, RAI Question No. 02.05.01-1  
(2) Summary of Regulatory Commitments

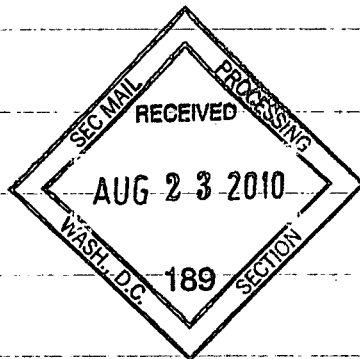
cc: USNRC, Director, Office of New Reactors/NRLPO (w/enclosure)  
USNRC, Project Manager, VCS, Division of New Reactor Licensing  
(w/enclosure)  
USNRC, Region IV, Regional Administrator (w/enclosure)

NP-10-0016  
Docket No. 52-042

**ENCLOSURE 1**

**Response to NRC RAI Letter No. 01**

**RAI Question 02.05.01-1**



**NRC RAI 02.05.01-1**

In FSAR Section 2.5.1.2.4.2.3 and 2.5.3.4.2 you describe growth fault D that breaks and offsets the current land surface and is located approximately 509 ft. to the southeast of the VC power block building. Growth fault E also breaks the surface but is farther away from the power block building. In accordance with Appendix C.2.4 and Regulatory Position 1.4 of Regulatory Guide 1.208, please provide the following information about the faults.

- a. Clarify the distance from Fault D to the planned power block area.
- b. Provide additional details on the movement history of growth fault D, including a justification for your assumption that the slip is continuous.
- c. Provide additional details on the calculation of slip-rate.
- d. Provide a discussion about your investigation on the age of the current land surface and the soil sequences over the surface expression of the fault.
- e. Provide a discussion about estimates of age of fault activity based on soil horizon evolution or soil catenas across the fault zone (McAlpin et al., 2009, p-251).
- f. Provide a discussion about the possible fault scarp at the surface. Include an estimate of time since last movement based on a fault scarp degradation analysis (McAlpin et al., 2009, p 247).

**Exelon Response**

This RAI question refers to growth faults D and E that were identified and described in the Victoria County Station (VCS) Site Safety Analysis Report (SSAR). The question describes the growth faults as breaking the surface and forming fault scarps, thus implying that the faults have caused a discrete offset or rupture of the surface. However, all of the data collected as part of VCS Early Site Permit (ESP) application (see SSAR Section 2.5.1.2.4.2.3) demonstrate that there is no evidence of either growth fault D or E breaking the surface or forming a fault scarp.

For example, based on interpretations of the seismic reflection data fault D offsets what is referred to as the Horizon 1 reflector. Above this horizon deformation is characterized by distributed folding (SSAR Section 2.5.1.2.4.2.3.1.4 paragraph 4). The lack of discrete surface offset or faulting associated with fault D is also confirmed by topographic profiles across the slope break. These profiles demonstrate that the land surface above the zone of distributed subsurface deformation is characterized by tilting or folding and not by discrete surface faulting (SSAR Section 2.5.1.2.4.2.3.2 paragraph 4). Topographic profiles demonstrate that the folding is associated with very low-relief separations of the Beaumont morphostratigraphic surface (order of several feet) over long distances (order of hundreds of feet) resulting in topographic breaks in slope with dips of less than 0.5° (SSAR Section 2.5.1.2.4.2.3.2 paragraph 3). Despite the fact that fault E is not imaged.

in the seismic reflection data (SSAR Section 2.5.1.2.4.2.3.1.3 paragraph 4), the similarity in surface morphology between fault D and E suggests that the surface deformation associated with fault E is also related to broad monoclinal folding or tilting and not discrete faulting (see SSAR Section 2.5.1.2.4.2.4). This style of broad warping is consistent with surface deformation associated with many growth faults throughout the Gulf Coastal plain (SSAR Section 2.5.1.2.4.2 paragraph 6).

As a point of clarification, the topographic profiles presented within the SSAR (SSAR Figures 2.5.1-48 and 2.5.1-50) are shown on plots with 100 to 200 times vertical exaggeration, and thus the broad monoclinal folding and tilting appear as abrupt changes in surface topography similar to erosionally modified fault scarps. However, when the same profiles are presented without any vertical exaggeration (Figure 1), the folding is not visibly discernable. When discussing the deformation associated with growth faults D and E, the profiles shown in the SSAR can be used to more easily identify the zone of deformation and assess its location and dimensions. However, the profiles presented in Figure 1 provide a more accurate representation of the true style of surface deformation above the buried growth faults.

Based on these observations regarding the expression of growth faults D and E, this response addresses the RAI question with respect to the monoclinal folding and surface tilting associated with faults D and E. To reiterate, this deformation is not expressed as surface breaks or scarps, neither of which is observed or documented within the data presented in the VCS ESP application (ESPA).

#### Issue a

The location of the zone of surface deformation associated with the folding and/or tilting of strata from movement on growth fault D relative to the ESP power block area is shown in SSAR Figure 2.5.1-43. As indicated in the figure, the closest approach is 155 m as measured between the southeast corner of the power block area and the northern extent of deformation (see SSAR Section 2.5.1.2.4.2.3). The area designated as the "power block area" in the VCS ESPA is a bounding power block layout conservatively established to envelope the area required for the power block buildings for each of the technologies evaluated in the ESPA. Therefore, the actual distance between the zone of deformation and any safety-related structure will likely be greater than 155 m.

No potential ground deformation associated with growth fault D is expected to approach closer to the power block area than the 155 m distance currently observed. This conclusion is based on the following:

- There is no deformation of the Beaumont surface within the power block area, indicating that there has been no surface deformation since formation of the upper Beaumont surface between 100,000 and 350,000 years ago (SSAR Section 2.5.1.2.4.2.3.3). Also, it is unlikely erosional processes have masked or removed any evidence of post-Beaumont surface deformation within the power block area because: (1) the small-scale, non-fluvial surface processes (e.g., sheet, rill, gully, and wind erosion as well as associated deposition) that are likely active in the area are generally thought to be a function of surface slope and curvature, with rates of these processes increasing with both greater slope and curvature (Easterbrook 1993). The average slope of Pleistocene deposits, approximately  $0.03^\circ$ , (Winker 1979)

and the increased slope from folding or tilting (i.e., less than 0.5° for fault D, see SSAR Section 2.5.1.2.4.2.3.2) within the site-area are very small (i.e., essentially zero) providing little to no topographic gradient or gravitational force to drive these geomorphic processes (Easterbrook 1993).

- The power block area is within the footwall of growth fault D, and this fault, as with all growth faults, has a listric form where the fault steepens as it approaches the surface (see SSAR Figures 2.5.1-45 through 2.5.1-48). The surface projection and zone of deformation associated with fault D has been documented as at least 155 m from the power block area. Based on the observed behavior of listric normal faults, in general, and growth faults in particular (e.g., Bally 1983; Nelson 1991; Watkins et al. 1996), it is unlikely that any deformation associated with fault D would propagate closer to the power block area.

Therefore, growth fault D does not pose a permanent ground deformation risk to the power block area.

#### Issue b

The movement history of growth fault D reflects a basic characteristic of growth faults in that displacement occurs during deposition of sediments that initially bury the fault, and which are subsequently deformed and offset by the fault. Consequently, the largest cumulative displacements are observed in the deepest and oldest portions of the sedimentary sequence affected by the faulting. The movement history of fault D can be reconstructed in part using the offset horizons identified in the seismic reflection data and the observed tilting/monoclinical folding of the land surface (see FSAR Figures 2.5.1-45 through 2.5.1-50 and Table 2.5.1-4):

- Growth fault D has produced approximately 1.5 to 4.5 ft of separation of the Beaumont geomorphic surface in the site-area in the form of broad monoclinical folding and tilting (see SSAR Section 2.5.1.2.4.2.3.2). This indicates that the vertical separation caused by the fault since deposition of the Beaumont Formation, estimated to have been between 100,000 and 350,000 years ago (SSAR Section 2.5.1.2.3), ranges between 1.5 to 4.5 ft (SSAR References 2.5.1-218, 2.5.1-132, 2.5.1-230, 2.5.1-40). The implied range in late Pleistocene slip rates, using the extreme values in separation and age, is between about  $5.4 \times 10^{-4}$  in/yr to  $5.1 \times 10^{-5}$  in/yr. Additional information regarding the age of the surface soil is provided in the response to Issue d, below.
- Growth fault D offsets seismic marker Horizon 4 between 66 and 72 ft (SSAR Table 2.5.1-4; Figures 2.5.1-45 and 2.5.1-47), but there is no age constraint on this horizon (see SSAR Section 2.5.1.2.4.2.3.1.2).
- Growth fault D offsets seismic marker Horizon 3 between 74 and 75 ft, only slightly more than the offset observed in Horizon 4 (SSAR Table 2.5.1-4; Figures 2.5.1-45 and 2.5.1-47). Horizon 3 is estimated to be a latest Miocene to Early Pliocene unit (i.e., about 5 million years old; see SSAR Section 2.5.1.2.4.2.3.1.2), so the offset of Horizon 3 indicates that there has been approximately 75 ft of vertical separation on growth fault D since the latest Miocene to Early Pliocene, implying a long-term average slip rate of about

$2.0 \times 10^{-4}$  in/yr since the late Neogene.

- Growth fault D offsets Horizon 2 identified in the seismic reflection data between 148 and 184 ft (SSAR Table 2.5.1-4; Figures 2.5.1-45 and 2.5.1-47). Horizon 2 is estimated to be the top of the Frio Formation, an Upper Oligocene to Lower Miocene formation (see SSAR Section 2.5.1.2.4.2.3.1.2), so the offsets in Horizon 2 indicate that there has been between approximately 148 and 184 ft of vertical separation on growth fault D since the Lower Miocene. Adopting an age of about 22 million years for the boundary between the Upper Oligocene and Lower Miocene (Salvador and Muneton 1991), the implied range in long-term average slip rate for Horizon 2 since early Neogene time is about  $8.1 \times 10^{-5}$  in/yr to  $1.0 \times 10^{-4}$  in/yr, bracketing the range in estimated separation of this horizon.
- Growth fault D offsets Horizon 1 identified in the seismic reflection data between 158 and 375 ft (SSAR Table 2.5.1-4; Figures 2.5.1-45 and 2.5.1-47). Horizon 1 is estimated to be the top of the Vicksburg Formation, a Lower Oligocene formation (see SSAR Section 2.5.1.2.4.2.3.1.2), so the offsets in Horizon 1 indicate that there has been between approximately 158 and 375 ft of vertical separation on growth fault D since the Lower Oligocene. Adopting a 30 Ma age for the Frio-Vicksburg boundary (Salvador and Muneton 1991), the implied long-term average separation rate of Horizon 1 is  $6.3 \times 10^{-5}$  in/yr to  $1.5 \times 10^{-4}$  in/yr.

There is evidence that growth fault E experienced movement during the Holocene based on the potential presence of monoclinial folding in Holocene flood plain deposits of the San Antonio River (see response to Issue d). Based on the Geomap data (SSAR Reference 2.5.1-123), growth fault E is a short splay of growth fault D (see SSAR Section 2.5.1.2.4.2.3). This structural relationship, combined with the similarity in surface expression of deformation associated with the two growth faults, could be interpreted as suggesting that post-Beaumont surface deformation occurred contemporaneously on both structures, and thus that the Holocene deformation associated with growth fault E could be used to indirectly estimate the Holocene separation rate on growth fault D. However, given the discontinuous nature of surface deformation associated with the growth faults (see SSAR Figure 2.5.1-37 and 2.5.1-44) relative to their subsurface extent (see SSAR Figure 2.5.1-36) (e.g., in general faults are significantly more extensive laterally in the subsurface than their surface expression), there is the potential that the surface deformation associated with growth faults D and E did not occur at the same time.

In calculating the potential slip rates that are discussed in SSAR Sections 2.5.1.2.4.2.3.3 and 2.5.1.2.4.2.4 for growth faults D and E, respectively, it is assumed that the slip has occurred continuously since the deposition of the offset stratigraphic horizons. This assumption was made as a matter of convenience in calculating potential long-term average, end-member separation rates (i.e., the rates presented in the SSAR are lower-bound estimates). As stated in the SSAR, it is possible that the observed cumulative deformation occurred through episodic slip events, and in this case the slip rates during periods of incremental deformation would be higher. Such short-term rates for episodic slip cannot be directly estimated for growth fault D because the Beaumont Formation is the only late Cenozoic stratigraphic marker that is deformed and whose age has been determined.

Issue c

Lower-bound, long-term average separation rate estimates are presented within the SSAR for both growth faults D and E (see SSAR Section 2.5.1.2.4.2.3.3 and 2.5.1.2.4.2.4, respectively). These are separation rates and not slip rates. To calculate formal slip rates on the fault planes, the dip of the faults needs to be taken into account.

As discussed in the SSAR, the separation rates are calculated using the “extremes in the range of relief and ages” of the separation of the Beaumont surface (see SSAR Section 2.5.1.2.4.2.3.3). For growth fault D, the separation observed in the Beaumont is between 1.5 ft and 4.5 ft. The age of the Beaumont Formation is between 100,000 years and 350,000 years. Using the extremes in both the ages and separation results in the separation rates presented in the SSAR as follows:

$$\bullet \frac{1.5 \text{ ft} \times 12 \frac{\text{in}}{\text{ft}}}{350,000 \text{ yrs}} = 5.1 \times 10^{-5} \frac{\text{in}}{\text{yr}}; \text{ and}$$

$$\bullet \frac{4.5 \text{ ft} \times 12 \frac{\text{in}}{\text{ft}}}{100,000 \text{ yrs}} = 5.4 \times 10^{-4} \frac{\text{in}}{\text{yr}}$$

For growth fault E, the separation observed in the Beaumont is approximately 4.9 ft. The age of the Beaumont Formation is between 100,000 years and 350,000 years. These values result in the separation rates presented in the SSAR as follows:

$$\bullet \frac{4.9 \text{ ft} \times 12 \frac{\text{in}}{\text{ft}}}{350,000 \text{ yrs}} = 1.7 \times 10^{-4} \frac{\text{in}}{\text{yr}}; \text{ and}$$

$$\bullet \frac{4.9 \text{ ft} \times 12 \frac{\text{in}}{\text{ft}}}{100,000 \text{ yrs}} = 5.9 \times 10^{-4} \frac{\text{in}}{\text{yr}}$$

Issue d

The primary formation of significance deformed by growth faults D and E is the Beaumont Formation. A complete discussion of the age of the Beaumont Formation is presented within SSAR Section 2.5.1.2.3, which describes the age of the Beaumont formation as being between 100,000 to 350,000 years old based on the current state of knowledge as represented in the scientific literature. No new age data were collected as part of the VCS ESP application to better constrain the age of the Beaumont Formation.

Additional information regarding the age of the surface disturbed by both growth faults D and E is described below.

#### *Growth Fault D*

Soil profiles typically exhibit characteristics that change systematically with the passage of time and have been used to estimate relative and absolute ages of land surfaces for neotectonic studies. Using published information, soil-geomorphic relationships were analyzed in the VCS-ESP site area. Soil sequences associated with the upper surface of the deformed Beaumont formation were compiled from existing published National Resources Conservation Service 1:24,000 soil maps and reports (Miller 1982; USDA 2010). New field-based soil investigations (e.g., pits, trenches) were not performed for the VCS ESP application because soil age will not be able to constrain the timing of deformation associated with growth fault D.

Soil map units observed and mapped in areas where there is deformation of the upper Beaumont surface associated with growth fault D include:

- Dacosta-Contee complex, 0 to 1 percent slopes;
- Faddin fine sandy loam, 0 to 1 percent slopes;
- Lake Charles/Laewest clay, 0 to 1 percent slopes; and
- Edna fine sandy loam, 0 to 1 percent slopes.

The Dacosta, Edna, Faddin, and Laewest soils are formed in deposits of the Pleistocene Beaumont Formation (Miller 1982; USDA 2010). Dacosta, Faddin, and Edna soils all have developed thick argillic layers (i.e., Bt horizons) ranging from 56 to 72 inches thick, and also possess accumulations of carbonates in the lowermost B horizon (e.g., Btk horizon). Clay coatings and clay films on ped faces also are present in the pedons (i.e., soil profiles). Laewest soils possess two Bk horizons (i.e., containing pedogenic carbonate). These characteristics generally indicate a pre-Holocene age of the land surface because the translocated clay horizons and accumulated discernable carbonate material as Bt or Bk horizons require landscape stability over relatively long times to develop (e.g., several tens of thousands of years).

The time to develop the observed soil profile characteristics does not provide any constraint on the timing of the currently observed deformation associated with growth fault D because soil development probably began upon cessation of the Beaumont formation and is not likely to have been impacted by the formation of the subtle monoclinical folding or tilting (e.g., steepest slopes of < 0.5°).

#### *Growth Fault E*

Based on soil survey maps, growth fault E traverses Pleistocene and Holocene age land surfaces (Miller 1982; USDA 2010).

Soil map units developed where there is deformation associated with growth fault E include:

- Dacosta-Contee complex, 0 to 1 percent slopes;
- Faddin fine sandy loam, 0 to 1 percent slopes;
- Lake Charles/Laewest clay, 0 to 1 percent slopes; and
- Edna fine sandy loam, 0 to 1 percent slopes.

At the southern end of the site area, the surface deformation associated with growth fault E extends into floodplain deposits of the San Antonio River (SSAR Figure 2.5.1-4 and 2.5.1-39). The floodplain surface is inset (topographically lower and younger) into the Beaumont Formation surface. Based on the NCRS soils map, the soils developed in the floodplain deposits are interpreted to be Holocene in age (USDA 2010). However, the site area geologic map included in the SSAR (SSAR Figure 2.5.1-4) incorrectly indicates that some of these deposits are of the Beaumont formation (i.e., the Qt map unit at the southern boundary of the site area in the San Antonio river valley). The site area geologic map and associated text within the SSAR will be modified, as described in the enclosed SSAR markups, to indicate that this unit is Holocene in age (i.e., the map unit will be described as Qal instead of Qt).

Soils interpreted to be Holocene in age on the floodplain surface include:

- Aransas clay, occasionally flooded, Aransas clay, frequently flooded;
- Rydolph silty clay, occasionally flooded;
- Sinton clay loam, occasionally flooded; and
- Trinity clay, frequently flooded.

None of the soils developed on the floodplain alluvium possess argillic (Bt) horizons suggesting insufficient time for substantial translocation of parent clay and therefore youthful soil horizons. The fact that each of the soils is flooded to some degree points to an active geomorphic floodplain surface with Holocene inundation and sedimentation.

Because the deformation associated with growth fault E appears to affect Holocene floodplain deposits, the most recent movement on growth fault E has occurred in the past 10,000 years.

#### Issue e

The variation in topography is so minor across the zone of surface deformation associated with both growth faults D and E (Figure 1) that the soils on the deformed surface would not be subjected to different rates or styles of soil-forming processes. Because different rates or styles are necessary to form a soil catena, variations in soil characteristics across the zone are not expected. The age of soil horizons on the tilted land surface are also not thought to be able to constrain the timing of deformation associated with the growth faults, because soil development is not likely to have been impacted by the formation of the subtle monoclinal folding or tilting (e.g., steepest slopes of  $< 0.5^\circ$ ). However, an analysis of soil maps for the site area (Miller 1982; USDA 2010) is described below.

Soil unit map boundaries over the surface deformation associated with growth fault D and E show no systematic pattern or map distribution that would indicate growth fault activity has influenced soil evolution (e.g., creation of slope and relief). Further, soil horizon descriptions of those units that overlie the surface expression of fault D support a generally Pleistocene age of soil establishment and development, but they do not constrain the timing of deformation beyond that provided by the age of the Beaumont Formation (see response to Issue d). Soil horizon descriptions of those units that overlie the surface expression of fault E support a Pleistocene age of soil establishment and development, and potentially a Holocene age for deposits topographically inset below the upper surface of the Beaumont Formation (see response to Issue d). As with growth

fault D, the soils do not constrain the timing of deformation beyond that provided by the age of the Beaumont Formation or potentially the Holocene floodplain deposits.

In addition, the available soil data (Miller 1982; USDA 2010) are insufficiently detailed to establish the presence of a catena (i.e., soil-topographic variations, thinning or truncating of horizons at scarp crest, contrasting soils at the scarp toe from ponding) within the broad zones of low-amplitude surface deformation associated with growth faults D and E. As stated previously, the magnitude of the variation in the slope across the zone of monoclinical folding and tilting is likely too small to produce any catena features.

#### Issue f

As discussed above, there is no observed fault scarp associated with either growth fault D or E. Instead, the faults are associated with broad, low-amplitude, monoclinical folding and/or tilting (Figure 1). As such, it is not appropriate or feasible to use diffusion dating, a method premised on the rate of erosional degradation of a scarp formed by discrete surface fault rupture, to estimate the age of the surface deformation. The primary reasons why diffusion dating and other methods cited in the reference provided in the RAI question (McCalpin 2009) are not appropriate include:

- There is no fault scarp. The topographic relief on the Beaumont surface above the growth faults was produced by long-wavelength tilting or folding, not erosion of a surface fault scarp, thus violating the key premise of the diffusion dating technique;
- The slope of the monoclinical folding and tilting is less than 0.5°, and is thus very gentle and not appropriate for the linear-plus-cubic diffusion method; and
- There are no reliable estimates of the diffusion constant for the type of Pleistocene sediments that comprise the Beaumont Formation and the climate of southern Texas; thus, it would not be possible to obtain reliable age estimates from the diffusion dating technique even if the Beaumont surface was deformed by discrete surface faulting.

Therefore, these methods are not applicable to dating surface tilting or folding due to slip on growth faults at depth, and thus are not appropriate for use in constraining the timing of deformation associated with the growth faults in the VCS site area.

**RAI Response References:**

Bally 1983. Bally, A.W., "Seismic Expression of Structural Styles, AAPG Studies in Geology," Volumes 1-3: Tulsa, OK, American Association of Petroleum Geologists, 1983.

Easterbrook 1993. Easterbrook, D.J., "Surface Processes and Landforms: New York, NY," 1993.

McCalpin 2009. McCalpin, J.P., "Paleoseismology," Second Edition, Academic Press, 2009.

Miller 1982. Miller, W.L., "Soil Survey of Victoria County Texas," Soil Conservation Service, US Department of Agriculture, 1982.

Nelson 1991. Nelson, T., salt tectonics and listric-normal faulting, in Salvador, A., ed., "The Geology of North America: the Gulf of Mexico Basin, Volume J: Boulder, CO," Geological Society of America, pgs. 73-89.

Salvador and Muneton 1991. Salvador, A., and Muneton, J.M.Q., Plate 5. Stratigraphic correlation chart, in Salvador, A., ed., "The Gulf of Mexico Basin, Volume J: Boulder," Geological Society of America.

USDA 2010. Web Soil Survey for Victoria County, available at <http://websoilsurvey.nrcs.usda.gov/app/HomePage.htm>, accessed on July 15, 2010.

Watkins et al 1996. Watkins, J.S., Bradshaw, B.E., Huh, S., Rong, L., and Zhang, J., Structure and Distribution of Growth Faults in the Northern Gulf of Mexico OCS, in Jones, J.O., and Freed, R.L., eds., "Structural Framework of the Northern Gulf of Mexico: Austin," Gulf Coast Association of Geological Societies, pgs. 63-73.

Winkler 1979. Winker, C.D., "Late Pleistocene Fluvial-Deltaic Deposition: Texas Coastal Plain and Shelf [MA thesis]: Austin, TX," University of Texas at Austin.

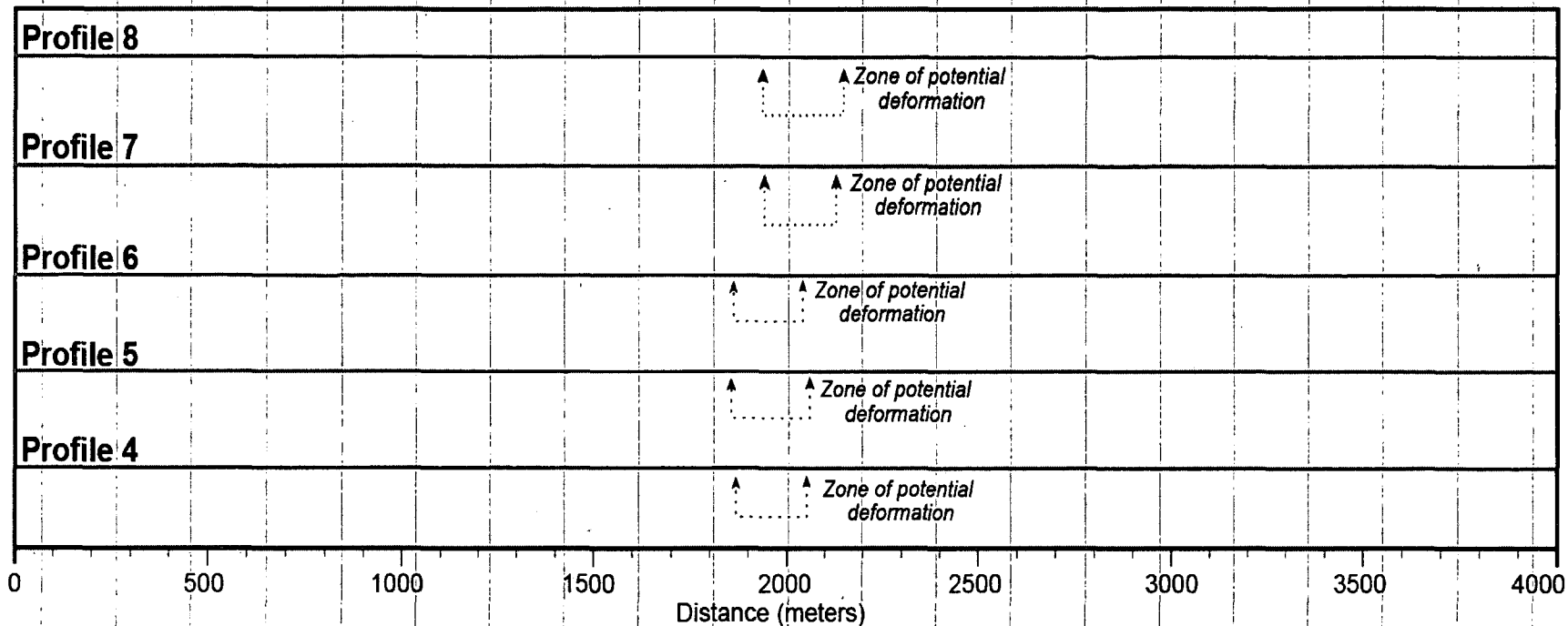


**Figure 1:** Profiles 4 through 8 from SSAR Figures 2.5.1-50b and 2.5.1-50c shown with no vertical exaggeration (i.e., 1:1 horizontal to vertical scale). Zones of potential deformation indicated in this figure are the same as in the original SSAR figures.

### Associated Proposed VCS ESP Application Revisions

SSAR Sections 2.5.1.2.4.2.3, 2.5.1.2.4.2.4, SSAR 2.5.1 References, and Figure 2.5.1-4 will be revised as follows:

The sixth paragraph of SSAR Section 2.5.1.2.4.2.3 will be revised as follows:

The topographic lineament of fault E is clearly discernable west of the San Antonio river valley, ~~and~~ cuts across an abandoned oxbow incised in the upper surface of the Beaumont Formation, and appears to cut across Holocene floodplain deposits based on the expression of the lineament within the LiDAR-derived topography and published soil maps (Reference 2.5.1-271). East of the San Antonio River valley, the LiDAR lineament splits into two short (approximately 0.25 mile or 0.4 km) branches with the lineament extending further east from between these branches (Figure 2.5.1-39). Immediately east of the fork the lineament is associated with a jog or deflection in the channel of Kuy Creek (Figure 2.5.1-39). Two short tributary branches of Kuy Creek appear to be just south of and aligned parallel to the lineament. Geologic field reconnaissance conducted for the VCS ESP application study confirmed the presence of the southeast-facing topographic break associated with accessible portions of the lineament. In particular, expression of the lineament is obvious where it crosses SR 239, FM 445, and between the crossing of the Kuy Creek main stem and the previously mentioned tributaries

The second paragraph of SSAR Section 2.5.1.2.4.2.4 will be revised as follows:

As described in Subsection 2.5.1.2.4.2.3, surface deformation associated with fault E is expressed in a variety of deposits and geomorphic surfaces ~~crosses a variety of features~~ including the deposits of the Beaumont Formation, younger Pleistocene and Holocene stream terrace deposits, and man-made features (i.e., FM 445, U.S. Highway 77, SR 239) (Figures 2.5.1-4 and 2.5.1-39). ~~Field reconnaissance of the fault across these features was unable to provide any refinements on the timing of activity other than that movement has occurred since deposition of the Beaumont, similar to the constraints on timing of fault D activity.~~ Topographic profiles of the fault along FM 445 derived from the LiDAR data reveal that the slope break associated with the fault has the same general characteristics as the non-degraded profiles of fault D (e.g., profile 4 and 8): a distinct inflection of the ground surface at the location of the lineament with the southeast side down. For fault E the relief across the tilted surface is approximately 4.9 feet (1.5 meters) over 980 feet (300 meters), or equivalently an increase in surface slope to approximately 0.29 degrees. ~~As with fault D, the age of the Beaumont Formation provides the only constraint on the rate of deformation for fault E. Again, assuming~~ Assuming the Beaumont was deposited between 350 ka and 100 ka, long-term deformation rates for fault E are between  $1.7 \times 10^{-4}$  inches per year and  $5.9 \times 10^{-4}$  inches per year. This vertical relief and implied deformation rates are similar to those observed for fault D. ~~If, as inferred~~

from the LiDAR-derived topography and soil maps (Reference 2.5.1-271), the deformation associated with the growth fault effects Holocene deposits, then long-term Holocene separation rates are approximately  $5.9 \times 10^{-3}$  inches per year. The apparently higher Holocene separation rate on fault E relative to the Pleistocene rate may be evidence for temporal variation in slip rate over time spans of thousands of years. The separation rates on fault D, estimated using multiple Tertiary stratigraphic markers extending the interval of deformation from about 100,000 years to 30 million years in age, are very similar; however, suggesting that slip rate is relatively uniform when averaged over hundreds of thousands to millions of years. ~~These~~ The morphological similarities between the two faults could either be coincidental or may suggest that the mechanisms, rates, and characteristics of growth fault activity within the site area are fairly uniform.

The following will be added to the references for SSAR 2.5.1:

2.5.1-271 Web Soil Survey for Victoria County, available at <http://websoilsurvey.nrcs.usda.gov/app/HomePage.htm>, accessed on July 15, 2010.

SSAR Figure 2.5.1-4 will be replaced with the following revised Figure:

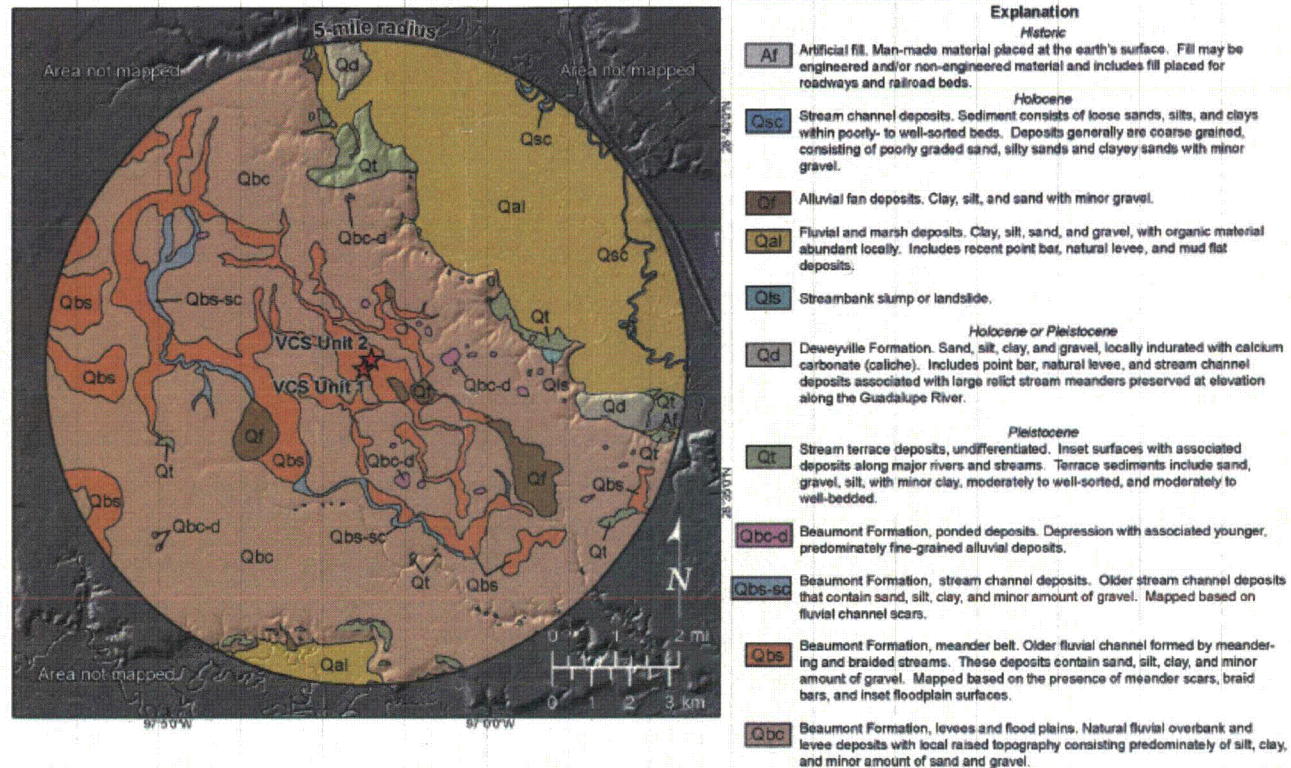


Figure 2.5.1-4 Site Area Geologic Map (5-Mile Radius)

Note: Shaded relief base from References 2.5.1-249 and 2.5.1-250.

**ENCLOSURE 2**

**SUMMARY OF REGULATORY COMMITMENTS**

**(Exelon Letter to USNRC, NP-10-0016, dated August 16, 2010)**

The following table identifies commitments made in this document. (Any other actions discussed in the submittal represent intended or planned actions. They are described to the NRC for the NRC's information and are not regulatory commitments.)

COMMITMENT	COMMITTED DATE	COMMITMENT TYPE	
		ONE-TIME ACTION (Yes/No)	Programmatic (Yes/No)
Exelon will revise the VCS ESPA SSAR Sections 2.5.1-2.4.2.3, 2.5.1.2.4.2.4, SSAR 2.5.1 References, and Figure 2.5.1-4 to incorporate the changes shown in Enclosure 1 in response to NRC RAI 02:05:01-1.	Revision 1 of the ESPA SSAR planned for March 25, 2011	Yes	No

